


## The Mott transition as a topological phase transition

Sudeshna Sen, Patrick J. Wong , and Andrew K. Mitchell <sup>\*</sup>  
*School of Physics, University College Dublin, Belfield, Dublin 4, Ireland*

 (Received 31 January 2020; revised 16 June 2020; accepted 31 July 2020; published 14 August 2020)

We show that the Mott metal-insulator transition in the standard one-band Hubbard model can be understood as a topological phase transition. Our approach is inspired by the observation that the midgap pole in the self-energy of a Mott insulator resembles the spectral pole of the localized surface state in a topological insulator. We use numerical renormalization-group–dynamical mean-field theory to solve the infinite-dimensional Hubbard model, and represent the resulting local self-energy in terms of the boundary Green's function of an auxiliary tight-binding chain without interactions. The auxiliary system is of generalized Su-Schrieffer-Heeger model type; the Mott transition corresponds to a dissociation of domain walls.

DOI: [10.1103/PhysRevB.102.081110](https://doi.org/10.1103/PhysRevB.102.081110)

**Introduction.** The Mott transition is a classic paradigm in the physics of strongly correlated electron systems, where electronic interactions drive a metal-insulator phase transition [1–3]. In a Mott insulator (MI), the strong local Coulomb repulsion localizes electrons, opening a charge gap to single-particle excitations and suppressing transport.

Although most MIs are accompanied by magnetic order at low temperatures, yielding a symmetry-broken superlattice structure [2], this is not an essential requirement [3–5]. The one-band Hubbard model on the Bethe lattice is the simplest model describing the Mott transition to a paramagnetic MI, and can be solved numerically exactly using dynamical mean-field theory (DMFT) [6,7]. The insulating properties of the MI cannot be understood on the single-particle level; all nontrivial physics is contained in the interaction self-energy [7–9]. Throughout the insulating phase, the MI self-energy features a midgap pole. In the metallic Fermi-liquid (FL) phase, Landau damping sets in at low energies. Close to the Mott transition, the FL self-energy develops a double-peak structure responsible for the preformed spectral gap, separating the central quasiparticle resonance in the density of states from the high-energy Hubbard bands. Importantly, the Mott transition from FL to MI arises without the gap between the Hubbard bands closing. At particle-hole symmetry (half filling), the self-energy peaks sharpen and coalesce to form a single Mott pole pinned at zero energy [7–9].

MIs contrast to standard band insulators, where the noninteracting band structure is already gapped due to the specific periodic structure of the real-space lattice. Indeed, the topology of the band structure of noninteracting systems plays an important role [10–12]. In particular, topological insulators constitute distinct phases of matter, characterized by robust metallic states localized at boundaries, or at interfaces with trivial insulators [13–15]. Topological phase transitions typically involve bulk gap closing without symmetry breaking, and are characterized by the discrete change in a topological

invariant [16]. However, for interacting systems the standard topological classification breaks down [17–19]. The effect of including electronic interactions in systems with topologically nontrivial single-particle band structures is the focus of active research [20–32].

Recently, the violation of Luttinger's theorem in correlated materials has been connected to the emergence of topological order [33–41]. Although Luttinger's theorem is satisfied throughout the FL phase of the Hubbard model due to the vanishing of the Luttinger integral [9,41–44], it is violated in a MI [9,42,45]. Importantly, the Luttinger integral takes a universal finite value throughout the MI phase [9], suggesting that it may play the role of a topological invariant, and that topological information is contained in the interaction self-energy.

In this Rapid Communication, we uncover a hidden topology in the self-energy of the standard one-band paramagnetic Hubbard model in infinite dimensions. Specifically, we show that the rich many-body features of the Mott transition can be interpreted in terms of topological properties of an auxiliary noninteracting system coupled to the physical lattice degrees of freedom. The original interacting lattice system is mapped onto a completely noninteracting one; the self-energy dynamics are provided by coupling to fictitious degrees of freedom of an auxiliary system (see Fig. 1). We use numerical renormalization-group (NRG) –DMFT [6,7,46] to calculate

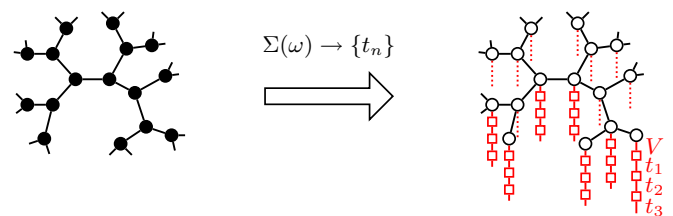


FIG. 1. Mapping from the Hubbard model (left) to a fully noninteracting system (right) in which physical degrees of freedom (○) couple to auxiliary tight-binding chains (□).

<sup>\*</sup>Corresponding author: [Andrew.Mitchell@UCD.ie](mailto:Andrew.Mitchell@UCD.ie)

the zero-temperature local lattice self-energy numerically exactly, perform the exact mapping to an auxiliary tight-binding chain coupled to each physical lattice site, and analyze their topological properties across the Mott transition. The auxiliary chains are found to be of generalized Su-Schrieffer-Heeger [47] (SSH) model type, with the MI being the topologically nontrivial phase. The double-peak structure of the self-energy in the topologically trivial FL phase corresponds to an SSH chain with additional domain walls. In each regime, we construct simple effective models to describe the emergent physics.

*Models and mappings.* To uncover the topological features of the Mott transition in their simplest form, we focus on the one-band Hubbard model (Fig. 1, left),

$$H_{\text{latt}} = H_{\text{band}} + H_{\text{int}} = \tilde{t} \sum_{\langle i,j \rangle, \sigma} c_{i\sigma}^\dagger c_{j\sigma} + U \sum_i c_{i\uparrow}^\dagger c_{i\uparrow} c_{i\downarrow}^\dagger c_{i\downarrow}, \quad (1)$$

where  $\langle i, j \rangle$  denotes nearest neighbors on the Bethe lattice. In the limit of infinite lattice coordination  $N \rightarrow \infty$  (considered hereafter), the self-energy  $\Sigma(\omega)$  becomes purely local [6] such that  $G(\omega) = 1/[\omega^+ - \Sigma(\omega) - t^2 G(\omega)]$ , where  $\omega^+ = \omega + i0^+$ ,  $t = \tilde{t}\sqrt{N}$ , and  $G(\omega)$  is the retarded lattice Green's function. We use NRG-DMFT [7,46] to determine  $\Sigma(\omega)$  at  $T = 0$  across the Mott transition.

Since the self-energy is analytic and causal, it may be replaced by a hybridization  $\Sigma(\omega) \equiv \Delta_0(\omega)$  to auxiliary (“ghost”) degrees of freedom described by some noninteracting  $H_{\text{aux}}$ . The full single-particle dynamics of Eq. (1) can therefore be reproduced by replacing  $H_{\text{int}} \rightarrow H_{\text{aux}} + H_{\text{hyb}}$ . Specifically, we take  $H_{\text{aux}}$  to be noninteracting semi-infinite tight-binding chains,

$$H_{\text{aux}} = \sum_{i,\sigma} \sum_{n=1}^{\infty} e_n f_{i\sigma,n}^\dagger f_{i\sigma,n} + t_n (f_{i\sigma,n}^\dagger f_{i\sigma,n+1} + \text{H.c.}), \quad (2)$$

coupled at one end to the physical lattice degrees of freedom,  $H_{\text{hyb}} = V \sum_{i,\sigma} (c_{i\sigma}^\dagger f_{i\sigma,1} + f_{i\sigma,1}^\dagger c_{i\sigma})$  [Fig. 1 (right)].

*Continued fraction expansion.* With  $H_{\text{aux}}$  in the form of a linear chain,  $\Delta_0(\omega)$  can be expressed as a continued fraction using  $\Delta_n(\omega) = t_n^2/[\omega^+ - e_{n+1} - \Delta_{n+1}(\omega)]$ , where  $t_0 = V$ . The set of chain parameters  $\{t_n\}$  and  $\{e_n\}$  in Eq. (2) for a given input self-energy  $\Sigma(\omega)$  is uniquely determined using this recursion for  $\Delta_n$  (initialized by  $\Delta_0 = \Sigma$ ), together with the identities  $t_n^2 = -\frac{1}{\pi} \text{Im} \int d\omega \Delta_n(\omega)$  and  $e_{n+1} = -\frac{1}{\pi t_n^2} \text{Im} \int d\omega \omega \Delta_n(\omega)$ . We impose a high-energy cutoff  $D$  such that  $\text{Im} \Sigma(\omega) \propto \theta(D - |\omega|)$  [48]. The mapping is efficient, numerically stable, and accurate, although care must be taken with poles in  $\Delta_n$  [49].

We now focus on the particle-hole symmetric (half-filled) case  $\mu = U/2$ , where  $\text{Im} \Sigma(\omega) = \text{Im} \Sigma(-\omega)$  and so  $e_n = 0$  for all sites of the auxiliary chain.

*Mott insulator.* For interaction strength  $U > U_c$ , the Hubbard model Eq. (1) describes a MI, with two Hubbard bands separated by a hard spectral gap of width  $2\delta$ . The corresponding self-energy at zero temperature is shown in Fig. 2(a), obtained by NRG-DMFT for  $U/t = 9$ . The imaginary part of the self-energy features a midgap “Mott pole” throughout the MI phase, pinned at  $\omega = 0$  (and with finite weight at the transition).

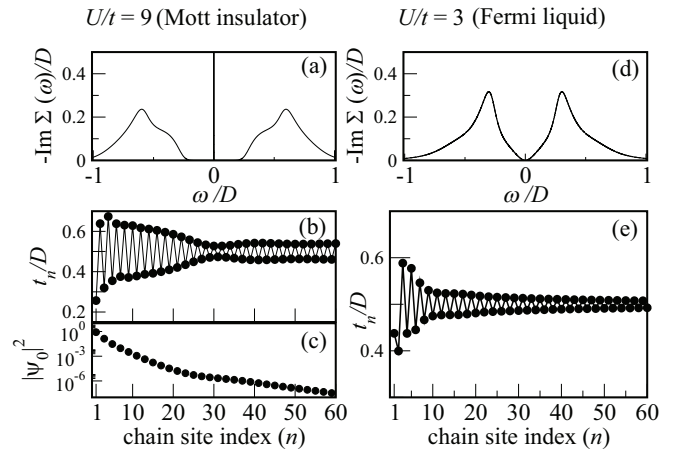


FIG. 2. Lattice self-energy at  $T = 0$  obtained from NRG-DMFT [panels (a) and (d)] and corresponding  $t_n$  of the auxiliary chain [panels (b) and (e)]. Left panels show results for the MI ( $U/t = 9$ ,  $D = 4$ ): the hard gap in  $\text{Im} \Sigma(\omega)$  and the Mott pole at  $\omega = 0$  produce an SSH-type chain in the topological phase, hosting an exponentially localized boundary zero mode, panel (c). Right panels show the metallic FL ( $U/t = 3$ ,  $D = 3$ ): the low-energy  $\omega^2$  pseudogap in  $\text{Im} \Sigma(\omega)$  produces a generalized SSH chain with  $1/n$  decay, in the trivial phase.

Mapping to the auxiliary noninteracting chain, Eq. (2), leads to a model of modified SSH type [see Fig. 2(b)]. In particular, the hard gap in  $\text{Im} \Sigma(\omega)$  generates an alternating sequence of  $t_n$  in  $H_{\text{aux}}$  at large distances from the physical degrees of freedom,

$$t_n \stackrel{n\delta/D \gg 1}{\sim} \frac{1}{2} [D + (-1)^n \delta] : \quad \text{MI} \quad (3)$$

In the MI phase, the auxiliary chain parameters are alternating for all  $n$ , starting from a weak bond ( $t_1 < t_2$ ). It is this feature that produces the Mott midgap pole at  $\omega = 0$ . Additional structure in the Hubbard bands merely gives rise to transient structure in the  $t_n$  for small  $n$ , but importantly the parity of the alternation,  $t_{2n-1}/t_{2n} < 1$ , is preserved for all  $n$  [see Fig. 2(b)].

The SSH model in its topological phase [Eq. (2) with  $t_n$  given by Eq. (3) for all  $n \geq 1$ ] hosts an exponentially localized boundary zero mode that is robust to parity-preserving perturbations [47]. Similarly, the zero-energy Mott pole corresponds to a robust and exponentially localized state living at the end of the auxiliary chain (on its boundary with the physical degrees of freedom of the original lattice). This can be readily seen from the transfer matrix method, which gives the wave-function amplitude of the zero-energy state at odd sites  $(2n - 1)$  of  $H_{\text{aux}}$  as  $|\psi_0(2n - 1)|^2 \sim \prod_{x=1}^n t_{2x-1}/t_{2x}$ , which at large  $n$  decays exponentially as  $\exp(-n/\xi)$  with  $\xi \approx D/2\delta$  for small  $\delta$  (while  $|\psi_0(2n)|^2 = 0$  for all  $n$ ) [47]. The boundary-localized nature of this zero-mode state is confirmed by exact diagonalization of  $H_{\text{aux}}$  [see Fig. 2(c)].

*Metallic FL phase.* For  $U < U_c$ , Eq. (1) describes a correlated metal, with low-energy FL properties characterized by a quadratic dependence of the self-energy,  $-\text{Im} \Sigma(\omega \rightarrow 0) \sim (\omega/Z)^2$ , in terms of the quasiparticle weight  $Z$ . In Fig. 2(d) we plot the  $T = 0$  self-energy deep in the FL phase, obtained by

NRG-DMFT for  $U/t = 3$ . We obtain a distinctive form for the auxiliary chain hopping parameters from the continued fraction expansion, arising due to the low-energy pseudogap in  $\text{Im}\Sigma(\omega)$ ,

$$t_n^2 \stackrel{nZ \gg 1}{\sim} \frac{D^2}{4} \left[ 1 - \frac{r}{n+d} (-1)^n \right]: \text{ FL}, \quad (4)$$

where  $r = 2$  is the exponent of the low-energy spectral power law, and  $d \sim 1/Z$ . Equation (2) with hopping parameters  $t_n$  given by Eq. (4) generalizes the standard hard-gapped SSH model to the pseudogapped case: the alternating sequence of  $t_n$  again has a definite parity, but with a decaying  $1/n$  envelope. Since  $t_{2n-1}/t_{2n} > 1$  for all  $n$  (the chain starting this time from a *strong* bond), the analogous SSH model would be in its trivial phase; likewise here, the FL phase of the Hubbard model may be regarded as trivial. There is no localized boundary state of the auxiliary chain in the FL phase.

*Vicinity of transition.* Deep in either MI or FL phases of the Hubbard model, the auxiliary chains are of generalized SSH model type, with the MI being topologically nontrivial. A robust and exponentially localized zero-energy state lives on the boundary between the auxiliary and physical systems throughout the MI phase, corresponding to the Mott pole. However, richer physics is observed on approaching the Mott transition from the FL phase. In particular, the Mott transition occurs *without* bulk gap closing of the Hubbard bands (unusual for a topological phase transition). What is the mechanism for the transition between the trivial FL and the topological MI in terms of the auxiliary chains?

In the vicinity of the transition on the FL side, the self-energy develops a preformed gap, inside which are peaks located at  $\pm\omega_p$  with  $\omega_p \propto t\sqrt{Z}$ , while quadratic ‘‘pseudogap’’ behavior sets in on the lowest-energy scales  $|\omega| \ll \omega_p$  [7–9]. The transition corresponds to  $Z \rightarrow 0$ . Before performing the exact mapping  $\Sigma(\omega) \rightarrow \{t_n\}$  numerically, we consider the evolution of chain parameters for a simpler toy system mimicking the Mott transition: two midgap spectral poles merging to one.

To do this, we consider the general problem of determining the chain parameters  $t_n$  for a composite spectrum  $A(\omega) = \frac{1}{\mathcal{N}} \sum_i w_i A_i(\omega)$ , with  $\mathcal{N} = \sum_i w_i$ . Although spectral elements are simply additive, the composition rule for the  $t_n$  is highly nonlinear. To make progress we note that spectral moments are additive,  $\mu_k = \frac{1}{\mathcal{N}} \sum_i w_i \mu_{i,k}$  with  $\mu_{i,k} = \int d\omega \omega^k A_i(\omega)$ , and use the moment expansion [50] of the chain parameters  $t_n^2 = X_n(n)$ , where

$$X_k(n) = \frac{X_k(n-1)}{t_{n-1}^2} - \frac{X_{k-1}(n-2)}{t_{n-2}^2}, \quad (5)$$

with  $X_k(0) = \mu_{2k}$ ,  $X_k(-1) = 0$ , and  $t_{-1}^2 = t_0^2 = 1$ .

Analysis of the equations shows that adding a zero-energy pole to the boundary spectral function of the SSH model in the trivial phase flips the parity of the corresponding  $t_n$  (the first coupling of the chain swaps from a strong to a weak bond), yielding the topological SSH model, Eq. (3), as expected. What change in  $t_n$  results from adding *two* poles at  $\pm\omega_p$  to the trivial SSH spectrum, as depicted in Fig. 3(a)?

Figures 3(c) and 3(d) show the chain parameters  $t_n$  for  $\omega_p/D = 10^{-2}$  and  $10^{-4}$ . At large  $n$ , the chain remains in

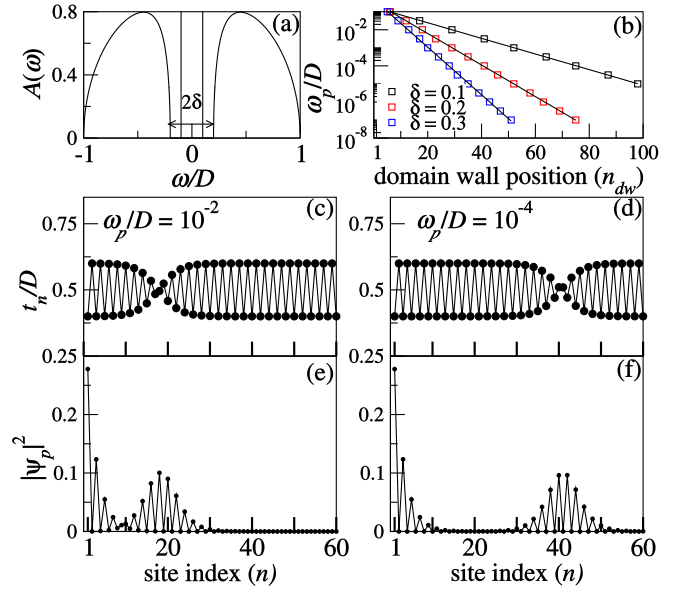


FIG. 3. Modified SSH model with two poles at  $\pm\omega_p$  inside a gap of width  $2\delta$  [spectral function illustrated in panel (a)]. Chain parameters  $t_n$  presented in panels (c) and (d) for  $\omega_p/D = 10^{-2}$  and  $10^{-4}$  with common  $\delta/D = 0.2$ , showing a domain wall at  $n_{\text{dw}}$ . States localized at the boundary and the domain wall hybridize and gap out to give exact eigenstates with energies  $\pm\omega_p$  [panels (e) and (f)]. The domain wall position [panel (b), points] follows  $\omega_p \sim D \exp(-n_{\text{dw}}\delta/D)$  (lines).

the trivial SSH phase. However, a domain wall appears at  $n_{\text{dw}}$  where the parity of the alternation flips; the chain for  $1 < n < n_{\text{dw}}$  is therefore in the *topological* phase of the SSH model (starting at  $n = 1$  from a *weak* bond). This produces *two* localized states: one at the boundary ( $n = 1$ ), and the other pinned at the domain wall ( $n = n_{\text{dw}}$ ), which hybridize and gap out to produce two states at energies  $\pm\omega_p$ . Since these are topological states and exponentially localized, the hybridization is exponentially small in the real-space separation between them along the chain, and we find  $\omega_p \sim D \exp(-n_{\text{dw}}\delta/D)$  [see panel (b)]. This physical picture is confirmed by examining the exact eigenstates  $\psi_p$  with energy  $\omega_p$  satisfying  $H_{\text{aux}}\psi_p = \omega_p\psi_p$ , plotted in panels (e) and (f).

The Mott transition as  $U \rightarrow U_c^-$  is characterized by  $\omega_p \rightarrow 0$ . In terms of the auxiliary chain, a *pair* of topological defects forms at the boundary when deep in the FL phase. One of these separates and moves down the chain as the transition is approached. As  $U \rightarrow U_c^-$ , then  $\omega_p \rightarrow 0$ , and  $n_{\text{dw}} \rightarrow \infty$ . At the transition itself, the two poles coalesce into the single Mott pole, and the chain is left with a single topological defect state at the boundary. This mechanism is reminiscent of the vortex-pair dissociation in the Kosterlitz-Thouless transition [51]. The topological transition occurs without bulk gap closing.

The behavior of the auxiliary chains for the actual Hubbard model is of course more complex than that of the above toy model. In particular, the true self-energy  $\Sigma(\omega)$  is not completely hard-gapped in the FL phase, but features a low-energy quadratic pseudogap. Including this leads to alternating  $t_n$  with a  $1/n$  envelope as per Eq. (4). Another key difference is that the peaks in the self-energy close to the transition are not delta

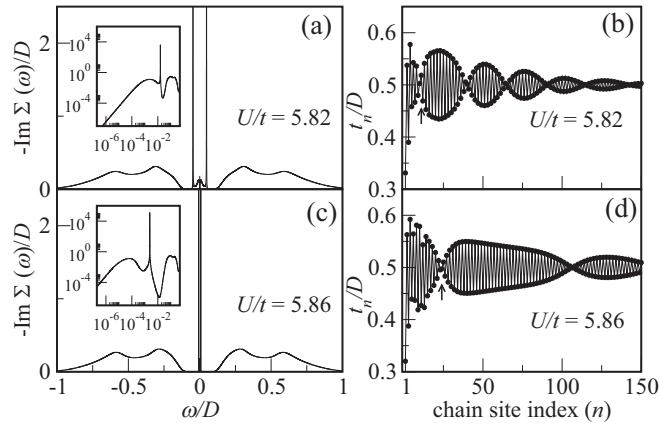


FIG. 4. Self-energy  $-\text{Im}\Sigma(\omega)$  from NRG-DMFT (a),(c) and corresponding auxiliary chain parameters  $t_n$  (b),(d) close to the Mott transition in the FL phase at  $T = 0$ . Top panels for  $U/t = 5.82$ ; lower panels for  $U/t = 5.86$  (both with  $D = 3$ ). Self-energy peaks of finite width centered on  $\pm\omega_p$  produce a generalized SSH chain with periodic domain wall structure. Low-energy  $\omega^2$  behavior of the self-energy manifests as long-distance  $(-1)^n/n$  behavior in the chains. As the transition is approached, the self-energy peaks sharpen into poles and  $\omega_p \rightarrow 0$ ; correspondingly, the location of the first domain wall moves out, and the beating period increases, leaving a single boundary-localized topological state in the MI.

functions but have finite width. For the auxiliary chains, these peaks can be viewed as narrow *bands* of hybridizing topological states produced by a periodic structure of domain walls, as shown in the Supplemental Material [49]. One therefore expects a beating pattern in the chain parameters.

All these expected features are seen in the exact results for the self-energy and corresponding chain parameters close to the transition, shown in Fig. 4. In particular, the chains start from a weak bond (giving a localized boundary state); the position of the first domain wall moves to larger distances as  $\omega_p$  becomes smaller nearer the transition; the period of the beating becomes longer as the self-energy peaks become sharper; and the alternation in  $t_n$  attenuates as  $1/n$  at long distances.

Combining these insights, we propose a simple toy model that approximates all of the qualitative features of the true lattice self-energy throughout the FL phase:

$$t_n^2 = \frac{D^2}{4} \left[ 1 - \frac{2}{n+d} (-1)^n \right] [1 - \beta \cos(2\pi n/\lambda + \phi)]. \quad (6)$$

A representative example is shown in Fig. 5(a), where we have fit the parameters of Eq. (6) to best match  $\Sigma(\omega)$  from NRG-DMFT [panel (c)] with  $\Delta_0(\omega)$  of the toy model [panel (b)]. The transition is approached as  $\lambda, d \rightarrow \infty$ .

*Particle-hole asymmetry.* We briefly comment on the physics away from particle-hole (*ph*) symmetry,  $\eta = 1 - 2\mu/U \neq 0$ . Throughout the MI phase, the Mott pole resides inside the hard gap between Hubbard bands, but is no longer at zero energy. The resulting auxiliary chain potentials  $e_n$  then become finite. We have confirmed in this case that the auxiliary chain state to which the Mott pole corresponds is still exponentially localized on the boundary, and is robust to physical perturbations (provided one remains in the MI

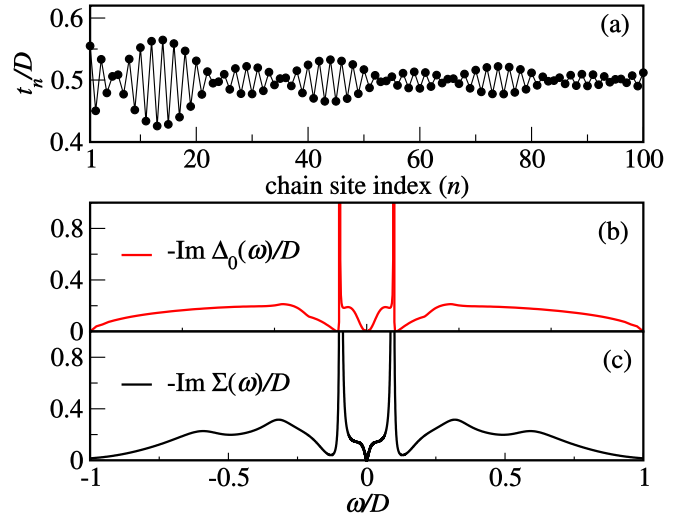


FIG. 5. Auxiliary chain parameters  $t_n$  of the toy model Eq. (6), with parameters  $\beta = 3$ ,  $d = 15$ ,  $\phi = 0.1$ , and  $\lambda = 30$  [panel (a)]. The resulting  $\Delta_0(\omega)$  [panel (b)] is in good agreement with the true lattice self-energy of the Hubbard model for  $U/t = 5.6$ ,  $D = 3$  [panel (c)].

phase). Furthermore, the analysis of Ref. [52] can be applied to the auxiliary chain. We again find that the MI is topologically nontrivial for  $\eta \neq 0$  (while FL is trivial). Everything is continuously connected to the *ph*-symmetric limit  $\eta \rightarrow 0$ . Further details and explicit calculations for  $\eta = 1/4$  are presented in the Supplemental Material [49]. A full discussion will appear elsewhere.

*Topological invariant.* A recent paper by Logan and Galpin [9] shows for the Hubbard model Eq. (1) at  $T = 0$  that the Luttinger integral takes distinct constant values in the FL and MI phases for any  $\eta \neq 0$  [53,54],

$$I_L = \frac{2}{\pi} \text{Im} \int_{-\infty}^0 d\omega G(\omega) \frac{d\Sigma(\omega)}{d\omega} = \begin{cases} 0 & \text{FL} \\ 1 & \text{MI} \end{cases} \quad (7)$$

The finite value of  $I_L$  for the generic MI can be traced to the Mott pole, which we identified in this work as the topological feature of the MI. Since the evolution of the self-energy with interaction strength drives the Mott transition, the Luttinger integral is a natural quantity to characterize the distinct topology of the FL and MI phases, and may be regarded as a topological invariant.

*Conclusions.* We present an interpretation of the classic Mott transition in the infinite-dimensional one-band Hubbard model as a topological phase transition. The lattice self-energy, determined here by NRG-DMFT, is mapped to an auxiliary tight-binding chain, which is found to be of generalized SSH model type. The MI is the topological phase, with a boundary-localized state corresponding to the Mott pole. The transition from FL to MI involves domain wall dissociation.

We argue that any system with such a pole in its local self-energy may be regarded as topological. The analysis could also be extended to multiband models, where the auxiliary chains become multilegged ladders. We speculate that a superconducting Hubbard model may map to auxiliary Kitaev chains involving Majoranas. For a fully

momentum-dependent self-energy of a  $D$ -dimensional lattice, the mapping generalizes to an auxiliary *lattice* in  $D + 1$  dimensions; for a MI, the auxiliary lattice may be a topological insulator with a localized boundary state.

*Acknowledgments.* We acknowledge discussions with Sidhartha Lal and N. S. Vidhyadhiraja. We acknowledge funding from the Irish Research Council Laureate Awards 2017/2018 through Grant No. IRCLA/2017/169.

- [1] J. Hubbard, *Proc. R. Soc. A* **276**, 238 (1963).
- [2] M. Imada, A. Fujimori, and Y. Tokura, *Rev. Mod. Phys.* **70**, 1039 (1998).
- [3] N. F. Mott, *Metal-Insulator Transitions* (Taylor and Francis, London, 1974).
- [4] V. Dobrosavljević, in *Conductor-Insulator Quantum Phase Transitions*, edited by V. Dobrosavljević, N. Trivedi, and J. M. Valles (Oxford University Press, Oxford, 2012), pp. 3–63.
- [5] A. Pustogow, M. Bories, A. Löhle, R. Rösslhuber, E. Zhukova, B. Gorshunov, S. Tomić, J. A. Schlueter, R. Hübner, T. Hiramatsu *et al.*, *Nat. Mater.* **17**, 773 (2018).
- [6] A. Georges, G. Kotliar, W. Krauth, and M. J. Rozenberg, *Rev. Mod. Phys.* **68**, 13 (1996).
- [7] R. Bulla, *Phys. Rev. Lett.* **83**, 136 (1999).
- [8] A. Georges and G. Kotliar, *Phys. Rev. Lett.* **84**, 3500 (2000).
- [9] D. E. Logan and M. R. Galpin, *J. Phys.: Condens. Matter* **28**, 025601 (2015).
- [10] M. Z. Hasan and C. L. Kane, *Rev. Mod. Phys.* **82**, 3045 (2010).
- [11] X.-L. Qi and S.-C. Zhang, *Rev. Mod. Phys.* **83**, 1057 (2011).
- [12] J. E. Moore, *Nature (London)* **464**, 194 (2010).
- [13] B.-J. Yang, M. S. Bahramy, and N. Nagaosa, *Nat. Commun.* **4**, 1524 (2013).
- [14] M. König, S. Wiedmann, C. Brüne, A. Roth, H. Buhmann, L. W. Molenkamp, X.-L. Qi, and S.-C. Zhang, *Science* **318**, 766 (2007).
- [15] D. Xiao, W. Zhu, Y. Ran, N. Nagaosa, and S. Okamoto, *Nat. Commun.* **2**, 596 (2011).
- [16] J. E. Moore and L. Balents, *Phys. Rev. B* **75**, 121306(R) (2007).
- [17] L. Fidkowski and A. Kitaev, *Phys. Rev. B* **81**, 134509 (2010); **83**, 075103 (2011).
- [18] T. Morimoto, A. Furusaki, and C. Mudry, *Phys. Rev. B* **92**, 125104 (2015).
- [19] L. Wang, H. Jiang, X. Dai, and X. C. Xie, *Phys. Rev. B* **85**, 235135 (2012).
- [20] S. Rachel, *Rep. Prog. Phys.* **81**, 116501 (2018); V. Y. Irkhin and Y. N. Skryabin, *Phys. Met. Metallogr.* **120**, 513 (2019).
- [21] L. Crippa, A. Amaricci, N. Wagner, G. Sangiovanni, J. Budich, and M. Capone, *Phys. Rev. Res.* **2**, 012023(R) (2020); A. Amaricci, L. Privitera, F. Petocchi, M. Capone, G. Sangiovanni, and B. Trauzettel, *Phys. Rev. B* **95**, 205120 (2017); A. Amaricci, J. C. Budich, M. Capone, B. Trauzettel, and G. Sangiovanni, *Phys. Rev. Lett.* **114**, 185701 (2015); *Phys. Rev. B* **93**, 235112 (2016).
- [22] M. Hohenadler and F. F. Assaad, *J. Phys.: Condens. Matter* **25**, 143201 (2013).
- [23] H.-H. Hung, V. Chua, L. Wang, and G. A. Fiete, *Phys. Rev. B* **89**, 235104 (2014).
- [24] J. M. Pizarro, S. Adler, K. Zantout, T. Mertz, P. Barone, R. Valentí, G. Sangiovanni, and T. O. Wehling, *arXiv:2001.04102*.
- [25] T. Yoshida, S. Fujimoto, and N. Kawakami, *Phys. Rev. B* **85**, 125113 (2012); Y. Tada, R. Peters, M. Oshikawa, A. Koga, N. Kawakami, and S. Fujimoto, *ibid.* **85**, 165138 (2012).
- [26] J. C. Budich, B. Trauzettel, and G. Sangiovanni, *Phys. Rev. B* **87**, 235104 (2013).
- [27] S. Raghu, X.-L. Qi, C. Honerkamp, and S.-C. Zhang, *Phys. Rev. Lett.* **100**, 156401 (2008).
- [28] P. Kumar, T. Mertz, and W. Hofstetter, *Phys. Rev. B* **94**, 115161 (2016).
- [29] A. Medhi, V. B. Shenoy, and H. R. Krishnamurthy, *Phys. Rev. B* **85**, 235449 (2012).
- [30] H. Ishida and A. Liebsch, *Phys. Rev. B* **90**, 205134 (2014).
- [31] M. Bijelic, R. Kaneko, C. Gros, and R. Valentí, *Phys. Rev. B* **97**, 125142 (2018); T. Yoshida, R. Peters, S. Fujimoto, and N. Kawakami, *Phys. Rev. Lett.* **112**, 196404 (2014); *Phys. Rev. B* **87**, 085134 (2013).
- [32] G. Magnifico, D. Vodola, E. Ercolessi, S. P. Kumar, M. Müller, and A. Bermudez, *Phys. Rev. D* **99**, 014503 (2019).
- [33] W. Wu, M. S. Scheurer, S. Chatterjee, S. Sachdev, A. Georges, and M. Ferrero, *Phys. Rev. X* **8**, 021048 (2018).
- [34] M. S. Scheurer, S. Chatterjee, W. Wu, M. Ferrero, A. Georges, and S. Sachdev, *Proc. Natl. Acad. Sci. USA* **115**, E3665 (2018).
- [35] S. Sachdev, *Rep. Prog. Phys.* **82**, 014001 (2018).
- [36] A. Paramekanti and A. Vishwanath, *Phys. Rev. B* **70**, 245118 (2004).
- [37] I. Osborne, T. Paiva, and N. Trivedi, *arXiv:2001.07197*.
- [38] T. Senthil, S. Sachdev, and M. Vojta, *Phys. Rev. Lett.* **90**, 216403 (2003).
- [39] V. Y. Irkhin and Y. N. Skryabin, *Phys. Lett. A* **383**, 2974 (2019).
- [40] A. Mukherjee and S. Lal, *New J. Phys.* **22**, 063007 (2020); **22**, 063008 (2020).
- [41] M. Oshikawa, *Phys. Rev. Lett.* **84**, 3370 (2000).
- [42] T. D. Stanescu, P. Phillips, and T.-P. Choy, *Phys. Rev. B* **75**, 104503 (2007).
- [43] I. Dzyaloshinskii, *Phys. Rev. B* **68**, 085113 (2003).
- [44] K. B. Dave, P. W. Phillips, and C. L. Kane, *Phys. Rev. Lett.* **110**, 090403 (2013).
- [45] A. Rosch, *Eur. Phys. J. B* **59**, 495 (2007).
- [46] A. Weichselbaum and J. von Delft, *Phys. Rev. Lett.* **99**, 076402 (2007).
- [47] W. P. Su, J. R. Schrieffer, and A. J. Heeger, *Phys. Rev. Lett.* **42**, 1698 (1979); J. K. Asbóth, L. Oroszlány, and A. Pályi, *A Short Course on Topological Insulators* (Springer, Cham, 2016).
- [48] Results presented are insensitive to the choice of  $D$ .
- [49] See Supplemental Material at <http://link.aps.org/supplemental/10.1103/PhysRevB.102.081110> for further details of (i) the continued fraction expansion of the self-energy; (ii) the moment expansion method; (iii) chain models with one or more midgap poles or peaks; (iv) NRG and DMFT calculations; and (v) the particle-hole asymmetric case, and which contains additional references [55–63].

- [50] V. S. Vishwanath and G. Müller, *The Recursion Method* (Springer, New York, 1994).
- [51] J. M. Kosterlitz and D. Thouless, *J. Phys. C* **5**, L124 (1972); **6**, 1181 (1973).
- [52] L. Li, Z. Xu, and S. Chen, *Phys. Rev. B* **89**, 085111 (2014).
- [53]  $\eta = 0$  is a special point at  $T = 0$  where the authors of Ref. [9] find  $I_L = 0$ . This appears to be an order-of-limits issue and  $I_L = 1$  in the MI is expected if  $\eta \rightarrow 0$  is taken before  $T \rightarrow 0$  [M. Galpin] (private communication).
- [54] For a detailed discussion of the Luttinger integral in non-Fermi liquid phases, see D. E. Logan, A. P. Tucker, and M. R. Galpin, *Phys. Rev. B* **90**, 075150 (2014).
- [55] J. P. Gaspard and F. Cyrot-Lackmann, *J. Phys. C* **6**, 3077 (1973).
- [56] W. Gautschi, *SIAM Rev.* **9**, 24 (1967).
- [57] K. G. Wilson, *Rev. Mod. Phys.* **47**, 773 (1975).
- [58] R. Bulla, T. A. Costi, and T. Pruschke, *Rev. Mod. Phys.* **80**, 395 (2008).
- [59] R. Žitko and T. Pruschke, *Phys. Rev. B* **79**, 085106 (2009).
- [60] A. Weichselbaum, *Ann. Phys.* **327**, 2972 (2012).
- [61] A. K. Mitchell, M. R. Galpin, S. Wilson-Fletcher, D. E. Logan, and R. Bulla, *Phys. Rev. B* **89**, 121105(R) (2014); K. M. Stadler, A. K. Mitchell, J. von Delft, and A. Weichselbaum, *ibid.* **93**, 235101 (2016).
- [62] A. K. Mitchell and R. Bulla, *Phys. Rev. B* **92**, 155101 (2015).
- [63] F. B. Anders and A. Schiller, *Phys. Rev. B* **74**, 245113 (2006).